Optical design of GIRMOS, an adaptive optics-fed integral-field spectrograph for the Gemini telescope

Tristan Chabot[a], Denis Brousseau[a], Shaojie Chen[b], Suresh Sivanandam[b], and Simon Thibault[a]

[a]Université Laval, 2325 rue de l'Université, Québec (Qc), Canada
[b]Dunlap Institute of Astronomy and Astrophysics, Toronto (Ontario), Canada

ABSTRACT

A conceptual design for GIRMOS (Gemini InfraRed Multi-Object Spectrograph) has been suggested to achieve a diffraction-limited instrument that will offer narrow band integral field spectroscopy (IFS) over the J, H and K bands of the NIR. It will also offer capabilities over three different fields of view (FOVs) and three different spatial sampling scales: 1.0"x1.0", 2.1"x2.1" and 4.2"x4.2", associated with samplings of 25 mas (mode 3), 50 mas (mode 2) and 100 mas (mode 3), respectively. Attainable resolutions are $R = 3000$ in all bands and all three observation modes, while the requirement $R = 8000$ is met in the K band for mode 1. The integral field unit is based on a 42 slices advanced image slicer concept. GIRMOS will consist of four identical integral field spectrographs (IFSes), each using its own 2k x 2k H2RG detector. This paper describes the conceptual optical design of GIRMOS, which successfully passed the conceptual design review that was held in Victoria in early September 2019.

Keywords: Infrared Instrumentation, Integral-field Spectrograph, Image Slicer, Multi-Object Adaptive Optics

1. INTRODUCTION

GIRMOS will be located at the Cassegrain focus of Gemini-South, using as input the MCAO diffraction-limited image quality provided by GeMS. A total of six spectral resolution settings of 3000 and 8000 are provided in all spatial scales, covering non-simultaneously the wavelength ranges that span the J, H and K bands, from 1.0 to 2.4μm. These observation modes are well matched to the diverse science cases that this instrument will address, from the study of kinematics at the center of the Milky Way to the structure and dynamics of distant galaxies.

A distinct feature of GIRMOS is that it will use simultaneously several integral field units covering the whole input focal plane, allowing better sky coverage. At the moment, four IFUs are planned, but the possibility of implementing twice as much might be studied in future design stages. The combination of these IFUs means that each one patrols a specific quadrant of the field of view, which is done by a pickoff system in the fore-optics of the instrument.

The bulk of the instrument lies inside a cryostat. Firstly, a fore-optics relay system provides the required F/# for the image slicer and focuses the input beam on it, while introducing an anamorphic ratio of 2. Three different paths are available; one for each mode. Therefore, this relay is used as the spatial scale mode selector. The image slicer divides the field of view into 42 slices which combine to form a single pseudo-slit as the spectrograph input. The latter is composed of a collimator lens, a stack of VPH gratings between two ZnSe prisms, and a camera. The grating choice is waveband dependant as well as the associated resolution setting. The prisms and the grating disperse light according to its wavelength and with the corresponding spectral resolution. Finally, the camera images the dispersed slit on the H2RG detector.

This paper focuses on the conceptual optical design of all the aforementioned subsystems of GIRMOS, from the focal plane of GeMS to the H2RG detector. This design was proposed at the GIRMOS conceptual design review held in September, 2019. Firstly, the optical design of the pickoff system is introduced. Then, anamorphosis in the fore-optics relay objectives is discussed and the three different designs are presented. The image slicer Integral Field Unit (IFU) is then described, along with fabrication considerations that are relevant to its design. Finally, the design of the spectrograph module is presented, with its optical and resolution performances, and a total throughput estimate is presented.

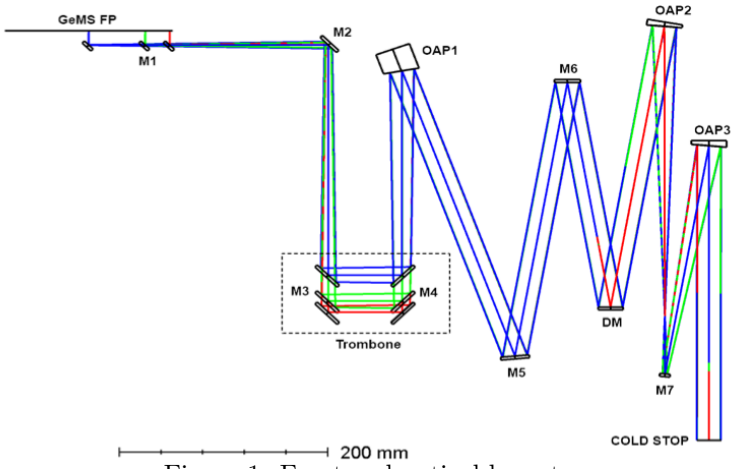

Figure 1: Front-end optical layout.

2. REQUIREMENTS

GIRMOS is being developed for the 8.1 m Gemini telescope, fed by the multi-conjugate adaptive optics F/33 beam of GeMS. It consists of four identical IFSes. Each IFS can pick off the FOVs at different spatial sampling scales and cover the J, H or K band with spectral resolutions of $R = 3000$ and $R = 8000$ depending on the spectrograph VPH. The requirements of the optical design of GIRMOS, derived from its sciences cases, are listed in table 1.

Table 1: GIRMOS top level optical design parameters.

Parameter	**Mode 1**	**Mode 2**	**Mode 3**
FOV [arcsec]	4.2 x 4.2	2.1 x 2.1	1.05 x 1.05
Sampling scale [mas]	100	50	25
Spectral resolution	3000 & 8000	3000 & 8000	3000 & 8000
Spectral range [μm]	1.1-2.4	1.1-2.4	1.1-2.4
Pixels per channel	2048 x 2048	2048 x 2048	2048 x 2048
Pixel size [μm]	18	18	18
Number of pixels/spectrum	2	2	2

3. PICKOFF SYSTEM

The first part of the fore-optics of the IFU design consist of a pickoff system which relays GeMS focal plane to the cryostat's cold stop, as illustrated at figure 1. It includes a deformable mirror (DM) and off-axis parabolas (OAPs) to create pupils having an identical diameter of 24 mm at both the DM and cold stop planes. The M1 mirror patrols GeMS focal plane, while the M3 and M4 trombone compensates pupil shift on the DM. Fold mirrors are also used because of the relatively small mechanical envelope available outside of the cryostat. The design consists entirely of reflective optics to minimize chromatic aberration at both the DM and the cold stop. The pickoff optics are replicated four times, one for each 1' patrolled quadrant. An important feature of the pickoff system is the ability to feed wavefronts that could be used by adaptive optics for correction. Therefore, knowing the wavefront error on the DM is important, as well as how much it may deteriorate when propagated to the cold stop. The corresponding results are shown in figure 2. Both surfaces are analyzed at the FFOV of 1'. The wavefront error on the DM is then 0.0982λ RMS and 0.4441λ peak-to-valley (PV). At the cold stop, the wavefront error is 0.0645λ RMS and 0.3000λ PV. These errors can easily be corrected by commercially available deformable mirrors.

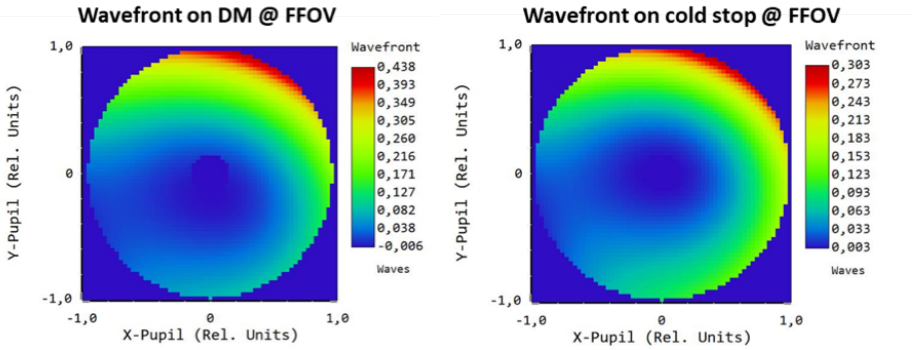

(a) (b)

Figure 2: Wavefront errors on the DM (a) and the cold stop (b), in waves at 1.65 μm.

4. ANAMORPHIC RELAYS

Optical relays are needed for the selection of the different spatial sampling scales (observation modes). Table 2 shows some basic calculations of the relay optics based on mode 2 requirements. As highlighted in red in the table, the height of the slit at the detector is too large by a factor of two in order to meet the 2 pixels slit width requirement at the detector , while completely covering the whole surface along the spatial axis. The optical relays from the cold stop to the slicer unit are thus designed with an anamorphic magnification of 2.

Table 2: Paraxial calculations.

Parameter	Variable	Units	Equation	Value
GeMS F/#	$F/\#_{GeMS}$			33.00
FOV (mode 2)	FOV	arcsec		2.10 x 2.10
FOV on GeMS FP (mode 2)	$HFOV_{GeMS}$	mm	$D \times F/\#_{GeMS} \times FOV \times (4.85 \times 10^{-3})$	2.722 x 2.722
Number of slices	N			42
Width of 1 slice on slicer	W_s	μm		250.000
Width of 1 slice on detector	W_d	μm	2 pixels	36.000
Width of slicer	W	mm	$N \times W_s$	10.500
Magnification from GeMS to slicer	M		W_s/W_{GeMS}	3.860
F/# on slicer for mode 2 (Dispersion axis)	$F/\#_{input}$		$M \times F/\#_{GeMS}$	127.200
Total magnification	M_T		W_s/W_{GeMS}	0.144
Height of slit on detector	H_s	mm	$N \times W \times M_t$	63.504
Height of slit with anamorphic mag. of 2	H_{AM}	mm	$N \times W/2 \times M_t$	31.752
F/# for mode 2 on H2RG	$F/\#_{cam}$		$M_t \times F/\#_{input}$	17.808

Figure 3 shows the anamorphic relay layouts for modes 1, 2 and 3. The relays are different in design but have an identical total track length of 1650 mm. Glasses with well-known cryogenic data and performances are used. Both spherical and toroidal surfaces are present in this design. The toroidal surfaces, on the last two elements of all three modes, introduce the anamorphic magnification. Output beams have focal ratios of F/63.6, F/127.2 and F/254.5 along the dispersion axis and for modes 1, 2 and 3, respectively.

Since the anamorphic relays focus light on the slicer so the field can be divided into 42 slitlets, the image quality on the slicer must be diffraction-limited to ensure good efficiency of the latter. Distortion should also be kept to a minimum to ensure there is no cross-talk between the slices and to maximize throughput at the edge slices. Distortion for modes 1 and 2 is not too significant, particularly in mode 1 where it is less than 0.15%. However, distortion in mode 3 could prove a problem, since it goes up to 4.7% at FFOV. Distortion should be maintained

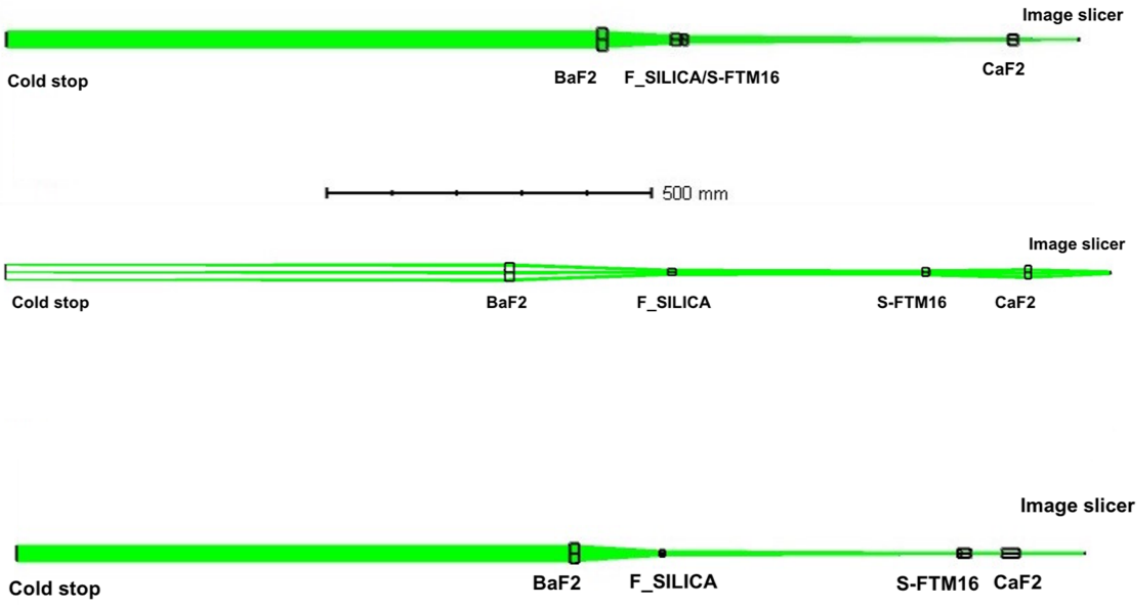

Figure 3: Optical layout of the anamorphic relays for modes 1 (top), 2 (middle) and 3 (bottom).

under 2.0% to minimize cross-talk between the edge slices. A 2.0% barrel distortion would make the edge of the FOV fall onto the neighboring slice, especially in mode 3 because of the large Airy spot size. Although this effect could be corrected in post-processing, further optimization in this regard could be done at later design stages to reduce the length of the post-processing pipeline.

As for image quality, all three modes are diffraction-limited on the image slicer array. As mentioned before, respecting the diffraction limit on the slicer's surface is important for efficiency reasons and for the overall instrument's image quality. The incident Airy spot size in mode 2 is of 512.11 μm at $\lambda = 1.65$ μm, while it measures 1024.21 mum in mode 3, also at a 1.65 μm wavelength. With the Airy spot size being already wider than the slit aperture in modes 2 and 3 because of the large F/#s, diffraction-limited PSFs help maximizing the throughput of the image slicer array and simplify the diffraction efficiency analysis that is required to assess this quantity.

5. IMAGE SLICER IFU

One of the most important parts of an Integral Field Spectograph (IFS) is the element that divides the field and creates the spectrograph's pseudo-slit. This component is called the Integral Field Unit (IFU) and may take the form of microlens arrays, fiber optics or image slicers. For GIRMOS, an image slicer concept has been chosen since it corresponds well to the requirements driven by the science cases of this project. Here, a 42 slices advanced image slicer concept is used, with each slice spanning a width of 250 mum, corresponding to a sampling of λ/D at $\lambda = 1.964$ μm. This mirror array spans a total width of 10.50 mm. The layout of the chosen advanced image slicer concept is shown in figure 4. The slicer design includes toroidal slices to compensate the pupil shift between the x and y axes that is introduced by the anamorphic optics. All other mirrors are spherical surfaces. Slices share the same radii of curvature in both axes, thus reducing fabrication complexity, while all other parameters of the IFU are allowed to vary. The pupil mirrors are arranged in two crescent-shaped rows and are powered to create a 108 mm long and 108 μm wide (mode 1) pseudo-slit on the corresponding field mirrors with a magnification of 0.42X. The field mirror array is also crescent-shaped, to ensure a constant magnification between each slice. The latter then form a common pupil on the VPH grating, at a distance of 500.00 mm from the central slices. Pushing the common exit pupil farther eases the optimization of the collimator lens because of the high incident angles on its entrance surfaces, but this distance is also limited by the tight packaging requirement within the cryostat, a cylinder of dimensions 1.0 m (D) x 1.2 m (L).

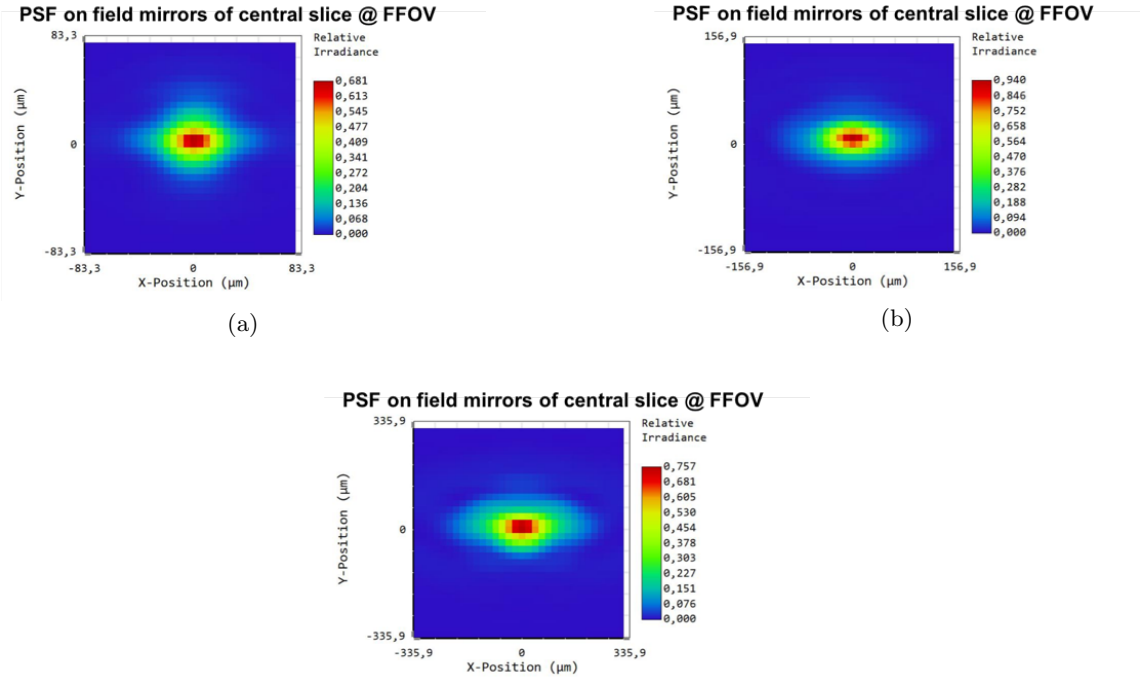

Figure 5: PSFs on the IFU field mirrors for mode 1 (a), mode 2 (b) and mode 3 (c). All three PSFs were measured at a 1.65 μm wavelength.

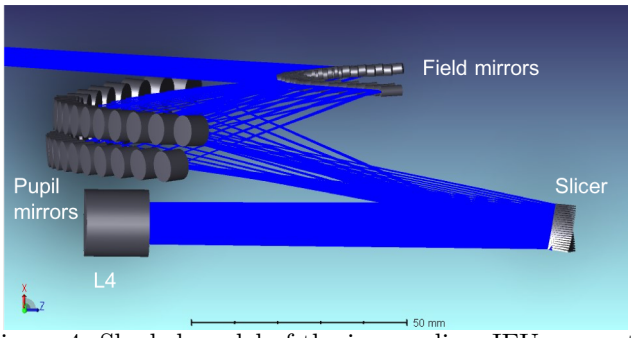

Figure 4: Shaded model of the image slicer IFU concept.

5.1 Image quality and efficiency

The image quality of the IFU is measured at the field mirror array, where the pseudo-slit is created. Sample PSFs, taken at the FFOV of GeMS, are shown in figure 5. Mode 1 is the most aberrated case, but can be compensated by the spectrograph optics, while modes 2 and 3 are diffraction-limited. A slight elongation of the PSF is observable in both of these modes, due to the slice aperture being two times to four times smaller than the incident Airy spot diameters at $\lambda = 1.65$ μm.

Diffraction efficiency is particularly important in image slicers design to estimate the total throughput of the IFU. Fourier optics simulations are used to propagate PSFs at different wavelengths and different spatial sampling scales on slice masks. Pupil mirror masks are then applied to measure the reflected illumination as a function of the mirror size relative to the elongated pupil. This analysis was applied to the design in all three modes. In mode 1, the pupil mirror size is about 1.62 times the pupil diameter, rendering a throughput of 85.85% in the J band, 85.62% in the H band, and 82.87% in the K band. In mode 2, the pupil mirror size is 1.95 times the pupil

diameter, allowing a throughput of 83.06% in the J band, 78.37% in the H band and 69.85% in the K band. In mode 3, because of the wider Airy spot, throughput losses are particularly important. Even with a pupil mirror size that is 2.2 times greater than the pupil size, the throughput falls to 69.42% in the J band, 56.14% in the H band and 43.26% in the K band.

5.2 Fabrication considerations

The main obstacle with advanced image slicer concepts lies in the manufacturing process. This is due to the number of surfaces and the rather small tolerances on each of the components. In the case of GIRMOS, all mirror arrays will be diamond turned from monolithic aluminum blocks, at AOFI (Advanced Optical Fabrication Infrastructure) of Université Laval. The individual parts will then be integrated into a complete IFU assembly, possibly using a bolt-and-go approach that has already been proven for the FISICA[1] project. The most challenging parts to manufacture will be the slicer stack and the field mirror array. Having slices with equal radii eases the process by reducing the number of variables to implement in the diamond turning program. The main restriction will be the dimension of the slices, but achieving good surface roughness on a 250 μm width is feasible using the right diamond tip size. Preliminary tests on 2.50 mm wide slices, using a tool radius of 0.775 mm and a step size of 10 μm, rendered a surface roughness of $R_q = 4.72$ nm and $R_a = 3.32$ nm. These results look promising for future fabrication work. RSA-6061 aluminum[2] could also be used to lower surface irregularities, considering that optimum diamond turning conditions can yield surface roughness values of $R_q = 1.0$ nm. If equal radii for the image slicer ease its fabrication, this consideration has the downside of complexifying the manufacturing process of the field mirror array. This part will be long and narrow, due to the small size of the mirrors (2.50 mm diameter) with regard to the 108 mm slit length. The curvature of the array also makes the diamond turning operation rather difficult if made from a single monolithic aluminum block. In this regard, diamond turning each mirror separately and assembling them mechanically could prove a better solution. Further investigation on this matter could be done at later design stages.

6. SPECTROGRAPH

The spectrograph optical design of GIRMOS is quite complex in its operation scheme. Since it uses three spectral bands and two resolution modes, each IFS unit consists of six different VPH gratings, for a total of 24 gratings for all the IFUs. The latter will be assembled between two ZnSe prisms to optimize cross-dispersion and maintain a straight optical axis. Mechanisms are needed to change those prism/grating assemblies. Other features of the spectrograph are the following:

- The same collimator and camera are used for all spectral bands and modes.
- Lenses are made of glasses for which cryogenic data is available.
- Lens surfaces are all spherical.
- Only cemented element is the prism/grating/prism (PGP) assembly, for cryogenic environment considerations.
- The collimator focal length is 450 mm and the camera focal length is 150 mm (1/3× magnification).

Table 3 shows the maximum achievable resolution in each spectral band. The calculation is based on the available dimensions on the H2RG detector (2k x 2k, 18 μm pixel size) and a target slit width of 2 pixels. Resolution in the K band is close to the $R = 8000$ requirement for a 2.1-2.4 μm wavelength range. However, in the J and H bands, the bandwidth would need to be reduced to achieve the $R = 8000$ requirement on this detector. The grating groove density would also need to be changed accordingly.

Table 3: Calculated maximum achievable resolutions on a H2RG detector.

Spectral band	**Wavelength range [μm]**	**R**
J	1.1-1.4	4167
H	1.5-1.8	5500
K	2.1-2.4	7500

Figures 6 and 7 show the layouts of the spectrograph elements and of the overall assembly. All elements are separated by air spaces of at least 1.0-mm thick, which is suitable for cryogenic environments. The collimator lens, in pair with the slicer IFU's field mirror array, forms a pupil on the VPH grating. The fourth Infrasil element of the camera serves as a field flattener, to compensate the field curvature that is introduced by the curved pseudo-slit.

The spectrograph optical design is based upon PGP (prism-grating-prism) assemblies which consist of a VPH grating stacked between two ZnSe prisms. Each grating consists of a layer of transmissive material sealed between two 3.0 mm thick layers of S-TIM35/S-BSL7. These materials were chosen for their CTE values which are similar to that of ZnSe. The resulting assembly is shown on figure 8. All six of these could be manufactured by Wasatch Photonics or Kaiser Optics.

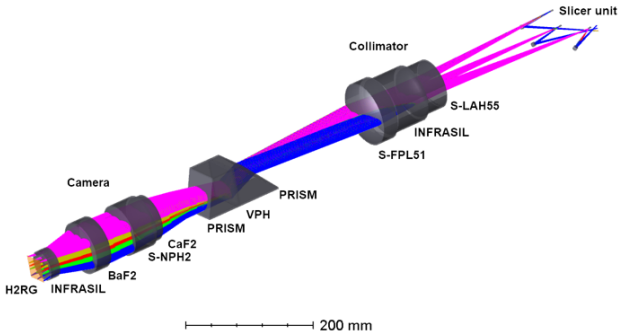

Figure 6: Spectrograph optical design layout. The center and two outermost slices rays are shown (K band, $R = 8000$).

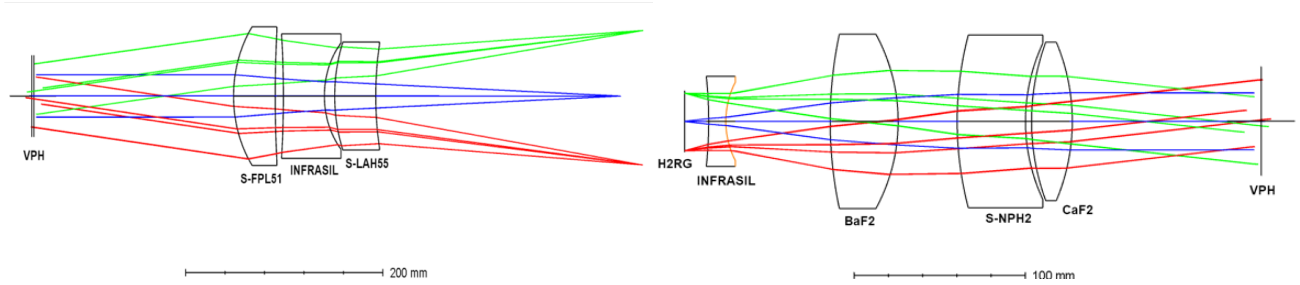

(a) (b)

Figure 7: Spectrograph collimator lens layout (a) and camera layout (b). The center and two outermost slices rays are shown (K band, $R = 8000$).

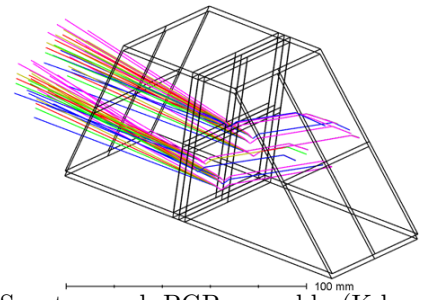

Figure 8: Spectrograph PGP assembly (K band, R=8000).

6.1 Image quality and resolution

Figure 9 shows the spectral distribution on the H2RG detector (mode 1) for each spectral band and both $R = 3000$ and $R = 8000$ targets, with the center and two outermost slices illustrated. The spectral distribution is the same for modes 2 and 3. Gratings have been optimized to cover a maximum area for the $R = 8000$ target. Table 4 shows the computed mean resolution in each spectral band assuming a uniform slit width of 2 pixels on the detector (mode 1). The calculation is made using the distance between the centroid positions of the minimum and maximum wavelengths of each spectral band on the detector. An average dispersion is then obtained and the resolution is calculated for the spectral band central wavelength. The computed resolutions at $R = 8000$ in mode 1 are close to the calculated limits of each band. The resolutions in modes 2 and 3 are calculated using each band's FWHM of the center slice at the central wavelength and on keeping the same spectrograph camera. Figure 10 shows FWHM cross-sections samples of a slitlet on the detector for mode 3. Note that the lobes of the cross-sections are caused by the diffraction of the slice, which is particularly significant in this mode. In order to reach $R = 8000$, the wavelength ranges would need to be reduced according to the values shown in table 5, along with different grating line densities.

Table 4: GIRMOS spectrograph resolution. Calculated resolutions are based on keeping the same spectrograph collimator and camera for all modes.

Spectral band [μm]	**R mode 1**	**R mode 2**	**R mode 3**
$R = 3000$			
$J = [1.1; 1.4]$	2989	2152	1344
$H = [1.5; 1.8]$	2858	2057	1286
$K = [2.1; 2.4]$	2938	2115	1322
$R = 8000$			
$J = [1.1; 1.4]$	3945	2840	1775
$H = [1.5; 1.8]$	5390	3880	2425
$K = [2.1; 2.4]$	7045	5072	3170

Table 5: Spectral range and VPH grating density required to achieve the $R = 8000$ goal.

Spectral band	**Spectral range [μm]**	**Grating density [l/mm]**
J	1.172 - 1.328	1000
H	1.547 - 1.753	750
K	2.110 - 2.390	550

7. THROUGHPUT

Considering the high number of surfaces in the current design, due to tight packaging restraints, throughput becomes an important issue. To maximize overall efficiency, all surfaces of the instrument should be coated according to material and environmental conditions. Therefore, all mirrors are proposed to be coated with bare gold, because of its high reflectivity over the targeted wavelength range, as shown in table 6. Moreover, it will not deteriorate in the uncontrolled environment of the front end of the cryostat. Bare silver has an even better reflectivity in the NIR, but deteriorates rapidly even within the limited exposure to the atmosphere that is involved in this application. Vapor deposition of gold, using an intermediate layer of chrome or nickel, is a proven technology that could also be applied to the image slicer, much like it was done for FRIDA,[3] for instance. Antireflection coatings should also be applied to lenses. Data from ISP Optics manufacturer indicate that the mean reflectivity of BaF2, Infrasil and S-FTM16 should attain a mean value of 0.75%, while the expected mean value for ZnSe equals approximately 0.30%.

The efficiency of the VPH gratings must also be considered. Figure 11, from Wasatch Photonics, shows sample diffraction efficiency curves for a VPH grating having 700 l/mm and optimized for the J band (left), and a VPH grating of 680 l/mm optimized for the K band (right). The average diffraction efficiency over the J band lies

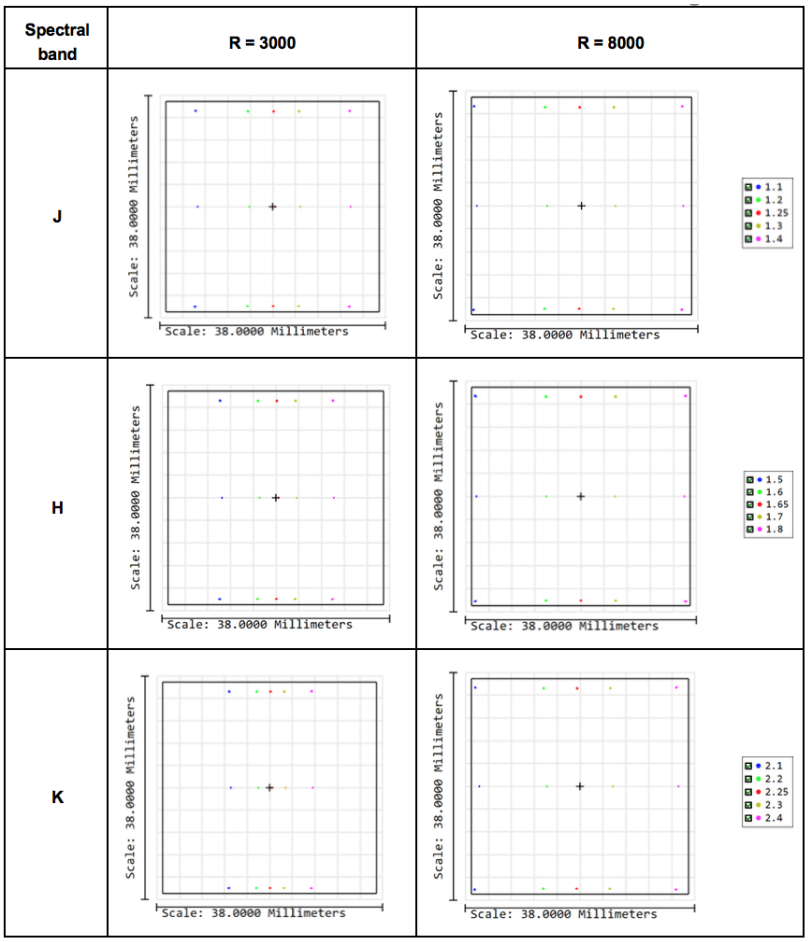

Figure 9: Distribution of the spectra on the H2RG detector in mode 1. The center and two outermost slices are shown.

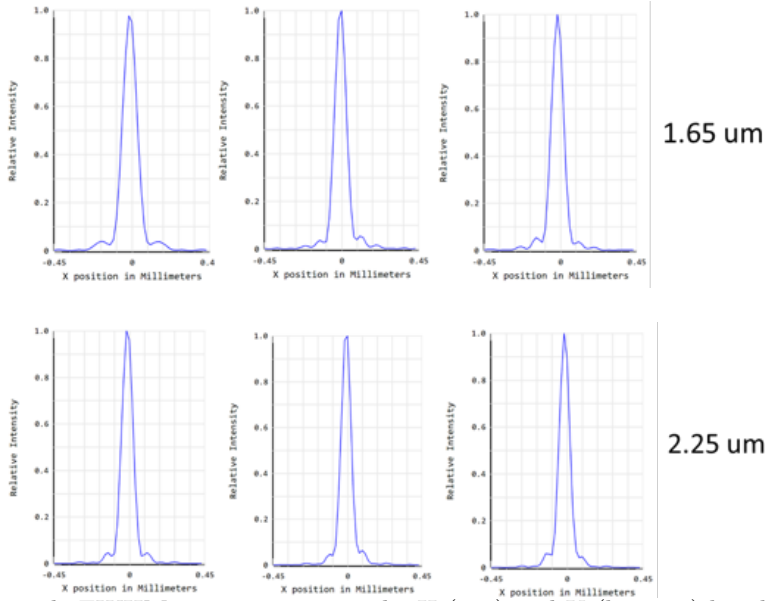

Figure 10: Sample FWHM cross-sections in the H (top) and K (bottom) bands, for mode 3.

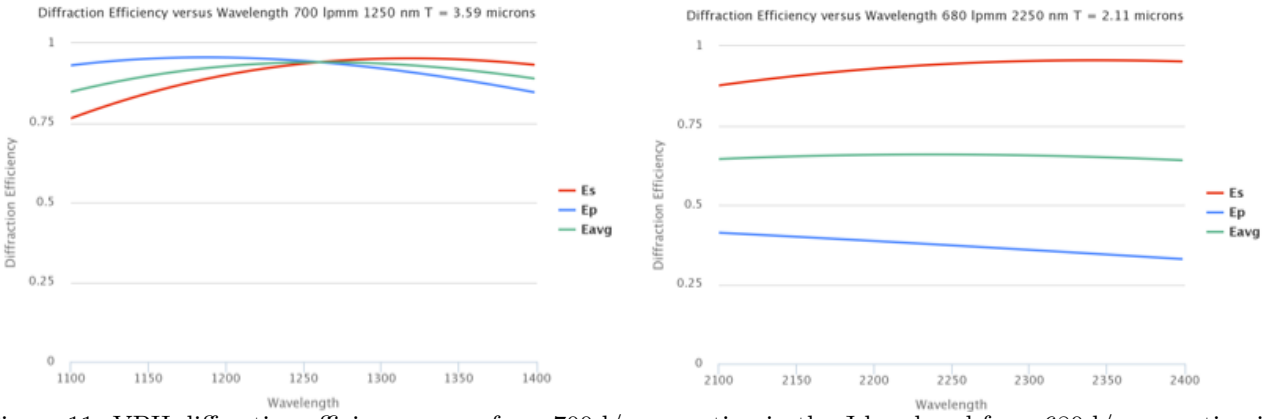

Figure 11: VPH diffraction efficiency curve for a 700 l/mm grating in the J band and for a 680 l/mm grating in the K band.

between 75% and 95%. Most of the gratings used in GIRMOS spectrograph's current design have efficiency curves similar to the one having 700 l/mm in the J band. However, the efficiency in the K band at $R = 8000$ is the lowest at an average value near 65%.

For a total throughput estimate, we considered a total of 24 mirror surfaces and 30 glass interfaces. Assuming an average reflectivity of 98.80% for the mirrors, 99.25% for the lens coatings and diffraction efficiencies of 72.72% and 60.00% for the slicer and the grating (respectively), we obtain an average throughput of 26.05%. Therefore, future design iterations must clearly focus on reducing the number of optical surfaces to improve the instrument's throughput.

Table 6: Reflectivity of vapor-deposited gold.

Wavelength [μm]	**Reflectivity [%]**
0.9	98.4
1.0	98.6
1.5	99.0
2.0	99.1
3.0	99.3

8. VERIFICATION OF SPECIFICATIONS

GIRMOS is presently at the conceptual design stage and is still in an early design phase. In this respect, the current version of the instrument shows satisfying image quality and resolution in modes 2 and 3 particularly. Nonetheless, further optimization of the outermost slices would be necessary to meet all requirements in mode 1.

The challenge with this instrument lies in the fact that four differents IFSes will be used simultaneously to make it a Multi-Object Spectrograph (MOS) that will not suffer from the usual light losses of a MOS spectrograph. This implies the use of either four different H2RG detectors or a single H4RG detector, which is twice the size of the former. H2RGs were chosen to minimize optical design difficulties, but the use of a single detector for all four IFUs might be necessary in the next design phases due to monetary considerations. This choice would probably allow for a better spectral resolution while limiting the costs, but would require more complex optics in the spectrograph.

ACKNOWLEDGMENTS

The authors would like to thank the Canada Foundation for Innovation for their financial involvement in this project.

REFERENCES

[1] Eikenberry, S., Raines, S. N., Gruel, N., Elston, R., Guzman, R., Julian, J., Boreman, G., Glenn, P., Hull-Allen, G., Hoffman, J., Rodgers, M., Thompson, K., Flint, S., Comstock, L., and Myrick, B., "FISICA: the Florida imager slicer for infrared cosmology and astrophysics," *Proc. SPIE* **6269**, 62694L (Jun 2006).

[2] Horst, R., de Haan, M., Gubbels, G., Senden, R., van Venrooy, B., and Hoogstrate, A., "Diamond turning and polishing tests on new rsp aluminum alloys," in [*Modern Technologies in Space- and Ground-based Telescopes and Instrumentation II*], *Proc. SPIE* **8450** (2012).

[3] Cuevas, S., Eikenberry, S. S., and Sánchez, B., "FRIDA integral field unit manufacturing," in [*Advances in Optical and Mechanical Technologies for Telescopes and Instrumentation*], *Proc. SPIE* **9151**, 91514N (Jul 2014).